IFSCC 2025 full paper (IFSCC2025-1172)

The Performance Comparison of *Thamnolia vermicularis* extract before and after Purification

Rong Tang[1*], Xiaoying Wan[1], Binfeng Zhang[1], Dan Liu[1], Meng Wang[1], Zichen Liu[1], Xiaolin-Tang[1], Minhua Hong[1]
1 Shanghai Peptide Biotechnology Co., Ltd, Shanghai, 201708, China

Abstract

Photoaging and glycation are major contributors to skin aging. In recent years, many natural ingredients have demonstrated good photoprotective and anti-glycation effects, indicating a broad application potential of natural ingredients in anti-aging. *Thamnolia vermicularis* (TV) is a traditional functional beverage and medicinal herb which thrives in the alpine snowscapes of China.TV exhibits pharmacological activities including anti-inflammatory, anti-senescence, and radioprotective which substantiates its therapeutic potential in oxidative stress-related pathologies. Currently, many commercial batches of TV are admixtures of TV and *Thamnolia subuliformis* (TS), but only the extract of *Thamnolia vermicularis* (TVE) is covered by Inventory of Existing Cosmetic Ingredients in China (IECIC) (2021). This study initially identified and analyzed TV and TS using UV and high-performance liquid chromatography (HPLC), revealing significant differences in their chemical compositions. The TVE was purified using an ion-exchange resins (ICE) to isolate its characteristic component, decarboxythamnolic acid (DA,Vermicularin). Comparative evaluation of the bioactivity variations in TVE before and after purification establishes a scientific foundation for optimizing its application in cosmetic formulations. Results showed that content of DA increased from 11.7% to 60.2% after purification. Both pre- and post-purification extracts demonstrated excellent anti-glycation, soothing, and repairing effects. However, the IC_{50} of DPPH assay scavenging was reduced by 14% after purification, indicating stronger antioxidant activity. The ability to inhibit melanin synthesis was also significantly enhanced after purification. Critically,

The TVE after purification demonstrates significant efficacy in suppressing MMP-3 overexpression induced by UV and preventing Type III collagen degradation, while TVE before purification exhibits no such biological activity. Thus, compared to TVE before purification, the TVE after purification had higher content of DA and improved anti-aging, photoprotective, and whitening effects.

Keywords

Thamnolia vermicularis extract, purification, performance comparison

1. Introduction

Photoaging and glycation are key factors leading to skin aging [1-2]. With consumers increasingly prioritizing rationality and safety in skincare, the gentle nature and eco-friendliness of natural ingredients have led to their growing prominence. At present, many natural ingredients have demonstrated good photoprotective and anti-glycation effects, indicating a broad application potential of natural ingredients in anti-aging [3-5].

Thamnolia vermicularis (TV) is the dried lichen thallus of *Thamnolia Vermicularis* (Sw.) Ach. It is primarily distributed in the snowy plateau regions of Tibet, Yunnan, Sichuan, and other high-altitude areas in China. With a long history of use, it is a traditional functional beverage and medicinal herb in Tibetan. In China, both TV and *Thamnolia subuliformis* (TS) are commonly referred to as "Snow Tea," and due to their similar appearance, many commercial raw materials are mixtures of the two. However, only the extract of *Thamnolia vermicularis* (TVE) is covered by Inventory of Existing Cosmetic Ingredients in China (IECIC) (2021). Therefore, the authentication of *TV* is essential before applying its extract in cosmetic products.

A few studies have reported the pharmacological effects of TVE. For example, Haiyuan YU [6] found that decarboxythamnolic acid (DA,Vermicularin) in TVE can inhibit MMP-1 production; Choi RY [7] reported that TVE can suppress adipocyte differentiation and reduce lipid accumulation. However, the photodamage repair and anti-glycation efficacy of TVE remain poorly documented in scientific literature.

Decarboxythamnolic acid (DA) is a characteristic constituent of TVE. Current literature predominantly employs organic solvents for the extraction of DA from TV, which poses risks

of residual chemical contamination and environmental sustainability concerns [6,8]. Thus, in this study, an ion-exchange resins (ICE) was utilized for DA purification. The adsorption of DA onto ICE significantly enhanced its concentration in TVE. Additionally, the higher content of DA can enhance the efficacy of TVE.

2. Materials and Methods

Materials: *Thamnolia vermicularis* was collected at Tibet, ion-exchange resins (Shanghai yuanye Bio-Technology Co., Ltd.), HDF-a cell, P815 cell, A375 cell (Shanghai Enzyme Linked Biotechnology Co., Ltd.), HFF cell (Guangzhou Boxi Biotechnology Co., Ltd.), Collagen Type III ELISA Kit ,MMP-3 ELISA Kit (NOVUS International, Inc.)**,** DPPH (AR), NaOH (AR), Decarboxythamnolic acid (≥94.9%,Laboratory-prepared).

Methods:

Identification of TV crude drugs

Weigh 0.5 g of TV and TS crude drugs, place them under UV light (UV5, Mettler-Toledo International Inc., Swiss.) and observe them under a wavelength of 365 nm.

Preparation of extracts from TV and TS crude drugs

The powders of TV and TS were treated with 0.28 mol/L NaOH solution (1:10 w/v) and ultrasonicated at 25°C for 0.5 h. The pH was adjusted to 2.76 using 0.1 M HCl solution under controlled stirring (1000 rpm/min)**.** After centrifugation (8,000 × g, 15 min, 25°C), the precipitate was dried under atmospheric pressure to obtain the final extracts.

Purification of TVE

Weigh an appropriate amount of TVE and dissolve in 0.28 mol/L NaOH solution to prepare a 0.03 g/mL (w/v) working solution. The solution was subjected to ICE column. The column was washed by deionized water and 1.73 M NaOH solution sequentially. The phase of deionized water containing unbound impurities was discarded, while the NaOH-eluted bioactive fraction was retained for subsequent processing. The alkaline eluate was acidified to pH 2.76 with 0.1 M HCl solution under controlled stirring (1000 rpm/min). After centrifugation (8,000 × g, 15 min, 25°C), the acid-insoluble precipitate was collected and dried under atmospheric pressure to yield the purified TVE.

Analysis of total phenolic acid

The same quality powders of TVE before and after purification and Extracts of TS (TSE) were weighed and dissolved with a DMSO-methanol solution (1:9, v/v) respectively, and the separation test and quantification were conducted using reversed-phase high -performance liquid chromatography (HPLC,1260 Infinity III, *Agilent Technologies Co, Ltd., USA.).* HPLC-DAD analysis conditions: Eclipse XB-C18 column (4.6 × 250 mm, 5 μm), detection wavelength 213 nm, column temperature 40 ℃, inject volume 10 μ L, flow rate: 1.0 mL/min.

DPPH assay

Transfer 1 mL of test sample solutions at varying concentrations into 15 mL amber tubes. Add 1 mL of freshly prepared DPPH solution (0.2 mg/mL in absolute ethanol) to each tube. Vortex mix (30 s at 2,500 rpm) and incubate in darkness at 25 ± 1°C for 20 min. Measure its absorbance A at 517 nm using microplate reader (SpectraMax iD3, Molecular Devices *Co, Ltd., USA*). Replace the DPPH solution with absolute ethanol to measure the absorbance A_1. Replace the sample solution with absolute ethanol to measure the absorbance A_0. The formula for calculating the DPPH assay using VC as a positive control is as follows:

DPPH free radical scavenging rate (%) $=A_0-（A-A_1）/A_0\times100\%$

Anti-aging test

HDF-a cells were diluted to a seeding density of 6×10^4 cells/well using complete culture medium and plated into 24-well plates (1 mL/well). After seeding, the plates were incubated in a humidified CO_2 incubator (5% CO_2, 37°C) for 24 h. Following incubation, the negative control group, positive control group, and test sample groups were irradiated with UVA at a total dose of 7 J/cm², while the blank control group remained unexposed.

Following irradiation, the culture medium was aspirated from all experimental groups. The blank control (BC) group and the negative control (NC)group were replenished with 1 mL of fresh complete growth medium per well. The positive control (PC) group received 1 mL of medium supplemented with 100 μg vitamin C and 7 μg vitamin E. For the sample groups, 1 mL of medium containing the designated concentrations of test compounds was added to each well. All plates were subsequently incubated under standardized culture conditions (5% CO_2, 37°C) for 24 hours to assess cellular recovery and treatment efficacy.

Following the completion of incubation, 1 mL of cell culture supernatant was collected from each well. Finally, the content of type Ⅲ collagen and MMP-3 was detected by ELISA kit.

Mast cell degranulation test

P815 cells in logarithmic growth phase were harvested and seeded into 24-well plates at a density of 2×10^5 cells/well. Post-seeding, the plates were transferred to a humidified CO_2 incubator (5% CO_2, 37°C) for 24 h.

BC group and NC groups were administered 1 mL of cell culture medium per well, while the PC group received medium supplemented with 100 μg/mL sodium cromoglicate. Sample groups were treated with 1 mL of medium containing their respective compound concentrations. All groups were incubated in a CO_2 incubator (5% CO_2, 37°C) for 24 h. After aspirating the supernatants, the BC group was replenished with 1 mL of fresh medium, and the remaining groups were exposed to medium containing 100 μg/mL compound C48/80. All groups were incubated in a CO_2 incubator (5% CO_2, 37°C) for 1 h. Reactions were immediately halted via immersion in an ice-water bath (0-4°C) for 10 min to ensure complete termination of cellular activity.

Cellular degranulation status across experimental groups was systematically evaluated using an inverted microscope (DMi8, Leica Microsystems Ltd., Germany). High-resolution micrographs were captured under phase-contrast mode to document morphological changes. Image-Pro Plus software (v6.0) was employed for quantitative analysis. The degranulation rate (%) was calculated using the formula:

Degranulation Rate (%) = [Total Degranulated Cells/ (Total Degranulated Cells + Total Non-Degranulated Cells)] ×100%

Anti-inflammatory test

RAW 264.5 cells in logarithmic growth phase were harvested and seeded into 24-well plates at a density of 1×10^5 cells/well. Post-seeding, the plates were transferred to a humidified CO_2 incubator (5% CO_2, 37°C) for 24 h.

The NC group was administered 1 mL of cell culture medium supplemented with 1 μ g/mL lipopolysaccharide (LPS) per well. The PC group received 1 mL of medium containing both 1

μ g/mL LPS and 0.1mg/mL dexamethasone. Sample groups were treated with 1 mL of medium containing 1 μg/mL LPS and the respective concentration of the test compound. All groups were incubated in a CO_2 incubator (5% CO_2, 37°C) for 24 hours.

Following the completion of incubation, 1 mL of cell culture supernatant was collected from each well. Finally, the content of IL-6 was detected by ELISA kit.

Cell scratch test

HSF cells in logarithmic growth phase were harvested and seeded into 24-well plates at a density of 1×10^5 cells/well. Post-seeding, the plates were transferred to a humidified CO_2 incubator (5% CO_2, 37°C) for 24 h. A sterile 200 μ L pipette tip was used to create a uniform linear scratch "wound" of HSF cell.

The NC group received 1 mL of basal culture medium per well. The PC group was supplemented with 1 mL of complete medium containing 10% FBS to simulate pro-growth conditions. Sample groups were treated with 1 mL of medium containing gradient concentrations of the test compound. All groups were incubated in a CO_2 incubator (5% CO_2, 37°C) for 24 h.

Cell migration was systematically evaluated using an inverted microscope (DMi8, Leica Microsystems Ltd., Germany). Images were analyzed with Image Pro Plus software (v6.0). The healing rate (%) was calculated using the formula:

Healing Rate (%) = [(*Initial Scratch Area – Current Scratch Area*) / *Initial Scratch Area*] × 100%.

Melanin inhibition test

A375 cells in logarithmic growth phase were harvested and seeded into 24-well plates at a density of 4×10^5 cells/well. Post-seeding, the plates were transferred to a humidified CO_2 incubator (5% CO_2, 37°C) for 24 h.

The BC group received 1 mL of basal cell culture medium per well. The PC group was treated with culture medium containing 0.01 mg/mL 377, while sample groups were supplemented with 1 mL of medium containing gradient concentrations of the test sample. All groups were incubated in a CO_2 incubator (5% CO_2, 37°C) for 24 hours.

Following incubation, the supernatant was aspirated, and 1 mL of 1 M NaOH containing 5% DMSO was added to each well. Plates were incubated at 60°C for 20 min to lyse cells and solubilize cellular components. The lysate supernatant was then transferred to a 96-well plate, and absorbance was measured at 490 nm using a microplate reader. The melanin inhibition rate was determined using the formula:

Melanin Inhibition Rate (%) = [(OD of BC group - OD of Sample group) / OD of BC group] × 100%

Anti-glycation test

HSF cells were diluted in cell culture medium to a density of 1×10^4 cells per well, seeded into a 24-well plate (1 mL per well), and cultured in a CO2 incubator (5% CO_2, 37°C) for 48 h.

After removing the culture medium, the NC group was treated with 1 mL of 0.3 mmol/L methylglyoxal working solution per well. The PC group received 1 mL of aminoguanidine sulfate working solution containing 0.3 mmol/L methylglyoxal, while the sample group was administered 1 mL of test sample solution with 0.3 mmol/L methylglyoxal. All groups were subsequently incubated in a CO_2 incubator (5% CO_2, 37°C) for 48 h.

Following incubation, the supernatant was aspirated and 1 mL of fixative solution was added to each well for 30 min at room temperature. After discarding the fixative, blocking buffer was applied for 1 h incubation at room temperature. The wells were then treated with primary antibody (diluted in PBS) for 2 h at room temperature, followed by three washes with PBS. Fluorescent-labeled secondary antibody was added for 1 h incubation in the dark. Post-wash, nuclei were counterstained with DAPI for 10 minutes. Imaging was performed using an inverted microscope, and integrated optical density was quantified via Image-Pro Plus 6.0 software with background subtraction. The AGEs inhibition rate was determined using the formula:

AGEs Inhibition Rate (%) = [(OD of BC group - OD of Sample group)/ OD of BC group] × 100%

Statistical analysis

The graphs were created using GraphPad Prism 9.0, and the result was expressed as Mean ± SD. t-test (two-tailed, $\alpha = 0.05$) was used for comparison between groups.

3. Results and discussion

Identification results of TV and TS

As shown in Figures (1a–1d), the appearance of TV and TS is similar under natural light. However, under 365 nm of UV light, TS exhibits yellow fluorescence while TV shows no fluorescence, which same as the findings of Wang J [9]. As shown in Figures 1e and 1f, the major depside components of TSE are squamatic acid and barbatic acid, whereas the main components in TVE are thamnolic acid and decarboxythamnolic acid (DA). The above results indicate that although *TV* and TS are morphologically similar and easily confused, their distinct chemical compositions provide a reliable basis for differentiating these two medicinal materials. As shown in Figures 1g, using laboratory-synthesized thamnolin as the reference standard, the content of DA in the TVE before purification was quantified at 11.7%**,** while the purified TVE achieved a purity of 60.2%. The content of DA was increase fivefold in TVE before purification which demonstrates robust adsorption-desorption interactions between TVE and ICE.

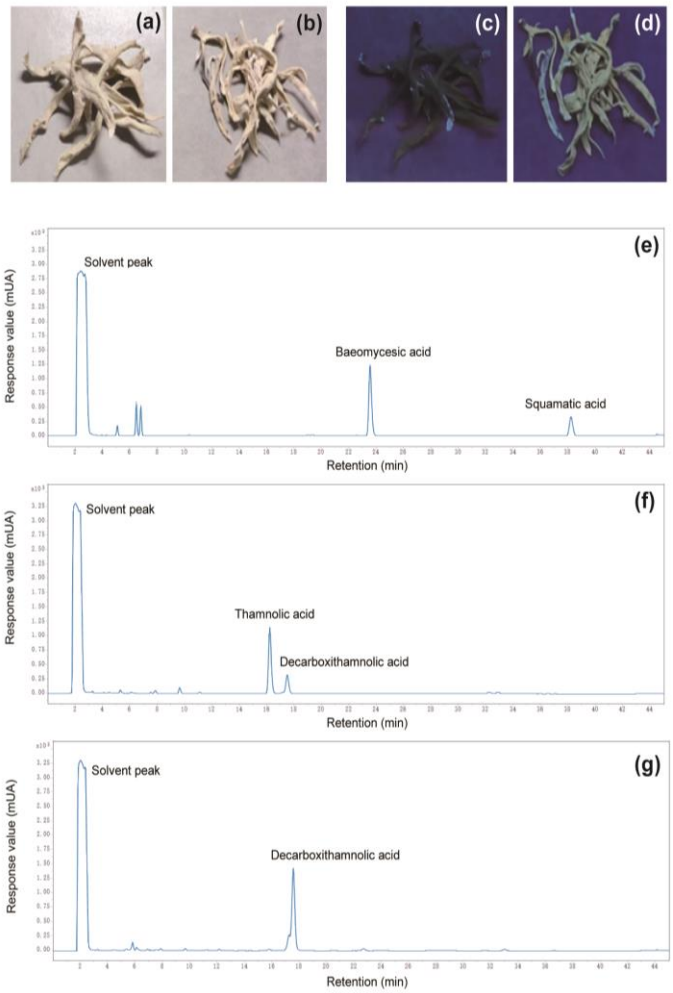

Figure 1. Identification and quantitative analysis results of TV. (a) Daylight image of TV. (b) Daylight image of TS. (c) UV image of TV. (d) UV image of TS. (e) HPLC chromatogram of TSE. (f) HPLC chromatogram of TVE before purification. (g) HPLC chromatogram of TVE after purification

Comparison of antioxidant and anti-aging effects of TVE before and after purification

Photoaging induces oxidative stress and excess free radicals, which damage intracellular proteins, DNA, and lipids, accelerating apoptosis [10]. DPPH is a widely used compound in radical scavenging assays, and a lower IC_{50} value indicates stronger antioxidant capacity [11]. As shown in Figure 2a, the IC_{50} of TVE before purification was 90.1 μg/mL, while that of TVE after purification was 77.7 μg/mL, representing a 14% decrease and significantly enhanced antioxidant activity.

Photoaging also leads to abnormal expression of MMPs, accelerating collagen degradation and causing wrinkles [12]. Type I and III collagens are the most abundant in the dermis. While prior studies have shown protective effects of TVE on type I collagen, its effect on type III collagen was previously unreported [6]. As shown in Figures (2b–2c), significant elevation of MMP-3 ($^{\#\#}P$<0.01) concurrent with reduced type III collagen concentration ($^{\#\#}P$<0.01) was observed in the NC group, which validated the effectiveness of the experimental model. At a concentration of 0.01 mg/mL, the TVE after purification demonstrated highly significant inhibition of MMP-3 secretion (**P<0.01) and marked stimulation of Type III collagen production (**P<0.01) in UV-irradiated HDF cells. In contrast, the TVE before purification exhibited no effects on either biomarker. These differences in antioxidant and anti-aging efficacy are likely due to the higher concentration of DA in TVE after purification.

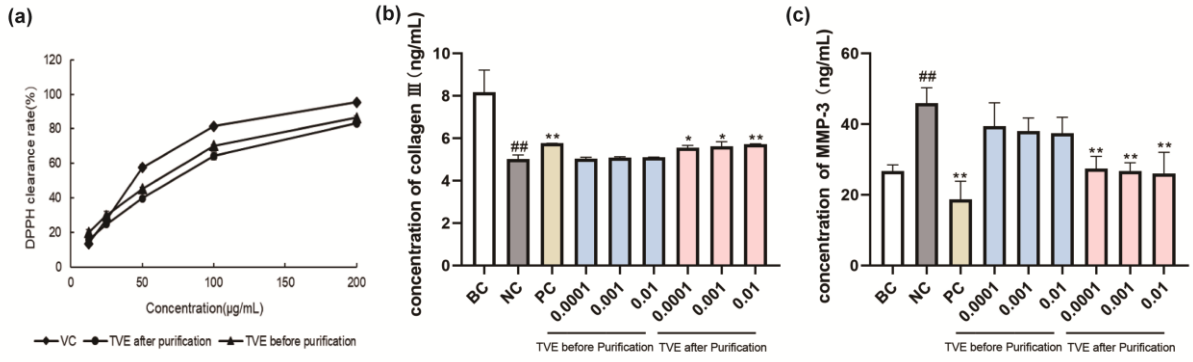

Figure 2. Results of antioxidant and anti-aging activities of TVE before and after purification. (a) Result of DPPH radical scavenging assay. (b) Result of Type III collagen synthesis assay. (c) Result of MMP-3 Inhibition Assay**.** $^{\#\#}$ $P < 0.01$ compare to the BC group, $^{*}P < 0.05$ and $^{**}P < 0.01$ compare to NC group.

Comparison of soothing, repairing, and whitening effects of TVE before and after purification

Prolonged UV exposure damages the skin barrier. To counteract photodamage, the skin's spontaneous repair mechanisms initiate a dual response: accelerated keratinocyte proliferation shortens the epidermal turnover cycle, while concurrently activating inflammatory pathways to release pro-inflammatory cytokines such as IL-6 and TNF-α. This compensatory process ultimately manifests as pathological hyperkeratosis and inflammation [13].

On the other hand, melanocytes secrete excessive melanin, which accumulates in the skin and leads to hyperpigmentation through increased epidermal melanin deposition [14]. Additionally, ultraviolet radiation upregulates endothelin expression, triggering mast cell degranulation and the release of histamine and other mediators, thereby inducing neurogenic inflammation characterized by sensory nerve activation and localized erythema [15-16].

As shown in Figures (3a–3c), significant elevation of degranulation rete and IL-6 concentration ($^{\#\#}P<0.01$) was observed in the NC group, which validated the effectiveness of the experimental model. At a concentration of 0.01 mg/mL, both TVE before and after purification significantly inhibited IL-6 secretion ($^{*}P<0.05$), suppressed mast cell degranulation ($^{***}P<0.001$), and enhanced healing rate of HSF cells ($^{\#\#\#}P<0.001$). These results demonstrate that TVE before and after purification both exhibit potent anti-inflammatory and tissue-reparative efficacy. As shown in Figure 3d, at 0.01 mg/mL, TVE after purification exhibited significantly stronger melanogenesis-inhibitory activity compared to TVE before purification ($^{\triangle}P < 0.05$), which demonstrates that the purification process can significantly enhance the whitening effect of TVE.

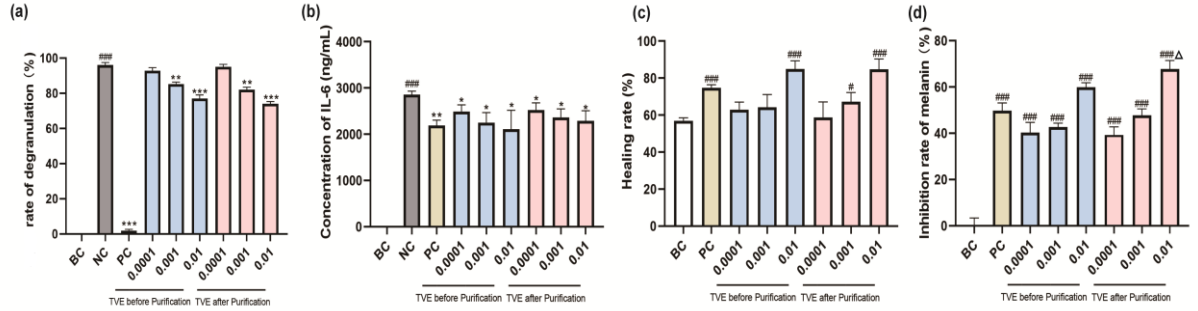

Figure 3. Results of the soothing, reparative, and capacities whitening effect of TVE before and after purification. (a) Result of Mast cell degranulation assay. (b) Result of IL-6 Inhibition Assay. (c) Result of fibroblast reparative rate. (d) Result of melanin Inhibition Assay. $^{\#}P < 0.05$ and $^{\#\#\#}P < 0.001$ compare to the BC group,$^{*}P < 0.05$ and $^{**}P < 0.01$ and $^{***}P < 0.001$ compare to the NC group, $^{\triangle}P < 0.05$ compare to the TVE before purification.

Comparison of anti-glycation effects of TVE before and after purification

Glycation reactions between sugars and dermal collagen form irreversible advanced glycation end products (AGEs), causing skin yellowing and dullness [17]. As shown in Figure 4, At a concentration of 0.01 mg/mL, both TVE before and after purification significantly anti-glycation effects ($^{\#\#\#}P<0.001$), with effects being concentration-dependent.

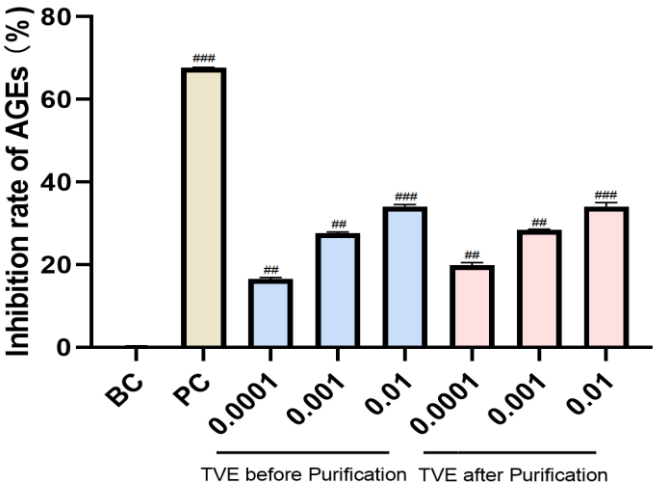

Figure 4. Result of anti-glycation activity of TVE before and after purification. $^{\#\#}P < 0.01$ and $^{\#\#\#}P < 0.001$ compare to the BC group.

4. Conclusion

Above all, UV lamper can distinguish between medicinal materials of TV and TS, while HPLC can differentiate TVE and TSE. The content of DA increased from 11.7% to 60.2% after purification via ICE. Both pre- and post-purification extracts demonstrated excellent anti-glycation, soothing, and repairing effects. However, the IC_{50} of DPPH assay scavenging was reduced by 14% after purification, indicating stronger antioxidant activity. The ability to inhibit melanin synthesis was also significantly enhanced after purification. Critically, The TVE after purification demonstrates significant efficacy in suppressing MMP-3 overexpression induced by UV and preventing Type III collagen degradation, while TVE before purification exhibits no such biological activity. Thus, compared to TVE before purification, the TVE after purification had higher content of DA and improved anti-aging, photoprotective, and whitening effects.

5. References:

1. Chan LKW, Lee KWA, Lee CH,et al (2024) Cosmeceuticals in photoaging: A review. Skin Res Technol. Skin res technol 30(9):e13730.

2. Guo Z, Li H, Jiang S, Rahmati M,et al (2025) The role of AGEs in muscle ageing and sarcopenia. Bone Joint Res 14(3):185-198.

3. Zheng Q, Jin X, Nguyen TTM, et al (2025) Autophagy-Enhancing Properties of *Hedyotis diffusa* Extracts in HaCaT Keratinocytes: Potential as an Anti-Photoaging Cosmetic Ingredient. Molecules 30(2):261.

4. Cano-Lou J, Millán-Laleona A, Candrea R, et al (2025) Apple peels as an edible source of phenolic bioactive compounds with antidiabetic and antiglycation properties. Food Funct 16(8):2947-2958.

5. Ávila F, Martinez N, Mora N, Márquez K, et al (2025) Effect of Thermal Treatment on the Extraction and Antioxidant and Antiglycation Activities of (Poly)phenols from *Ribes magellanicum*. Molecules 30(2):318.

6. Choi RY, Ham JR, Yeo J, et al (2017) Anti-Obesity Property of Lichen *Thamnolia vermicularis* Extract in 3T3-L1 Cells and Diet-Induced Obese Mice. Prev Nutr Food Sci 22(4):285-292.

7. Haiyuan YU, Shen X, Liu D, et al (2019) The protective effects of β-sitosterol and vermicularin from Thamnolia vermicularis (Sw.) Ach. against skin aging in vitro. An Acad Bras Cienc 91(4):e20181088.

8. Guo J, Li ZL, Wang AL, Liu XQ, et al (2011) Three new phenolic compounds from the lichen Thamnolia vermicularis and their antiproliferative effects in prostate cancer cells. Planta Med 77(18):2042-6.

9. Wang J, Zhao H, Guo Q, et al (2022) Identification and antibacterial activity of Thamnolia vermicularis and Thamnolia subuliformis. J Microbiol Methods. 203:106628.

10. Gu Y, Han J, Jiang C, Zhang Y (2011) Biomarkers, oxidative stress and autophagy in skin aging. Ageing Res Rev 59:101036.

11. Akbar A, Soekamto N H, Firdaus, et al (2021) *Antioxidant of n-hexane,* ethyl acetate and methanol extracts of Padina sp with DPPH method. IOP Conference Series: Earth and Environmental Science 800(1), 012019.

12. Li F, Zhi J, Zhao R, Sun Y, et al (2024). Discovery of matrix metalloproteinase inhibitors as anti-skin photoaging agents. Eur J Med Chem 267:116152.

13.Zheng Q, Yang SJ, Yi EJ, et al (2025) Enzyme-assisted Rosa davurica mitigates UV-induced skin photodamage by modulating apoptosis through Nrf2/ARE and MAPK/NF-κB pathways. J Photochem Photobiol B 263:113098.

14. Vachiramon V, Kositkuljorn C, Leerunyakul K, et al (2021) A Study of Botulinum Toxin A for Ultraviolet-Induced Hyperpigmentation: A Randomized Controlled Trial. Dermatol Surg 47(5):e174-e178.

15. Leis Ayres E, Dos Santos Silva J, Eberlin S, et al (2022) Invitro effect of pine bark extract on melanin synthesis, tyrosinase activity, production of endothelin-1, and PPAR in cultured melanocytes exposed to Ultraviolet, Infrared, and Visible light radiation. J Cosmet Dermatol 21(3):1234-1242.

16. Trentin Brum S, Demasi AP, Fantelli Stelini R, et al (2019) Endoglin is Highly Expressed in Human Mast Cells. Appl Immunohistochem Mol Morphol 27(8):613-617.

17. Wang L, Jiang Y, Zhao C, et al (2024) The effects of advanced glycation end-products on skin and potential anti-glycation strategies. Exp Dermatol 33(4):e15065.